Superscripts

I = matrix or continuous phase
II = filler or disperse phase
$*$ = new policy in the iteration scheme

LITERATURE CITED

1. Cheng, S. C., and R. I. Vachon, *Intern. J. Heat Mass Transfer*, **12**, 249 (1969).
2. Gorring, R. L., and S. W. Churchill, *Chem. Eng. Progr.*, **57** (7), 53-59 (1961).
3. Woodside, W., and J. H. Messmer, *J. Appl. Phys.*, **32** (9), 1688-1706 (1961).
4. Griffis, C. L., N. C. Nahas, and J. R. Couper, *Univ. Arkansas Eng. Exp. Sta. Res. Rept. No. 5* (1964).
5. Deissler, R. G. and C. S. Eian, *NACA RM E52C05* (1952).
6. Krupiczka, R., *Intern. Chem. Eng.*, **7** (1), 122 (1967).
7. Hashin, Z., *J. Composite Materials*, **2** (3), 284 (1968).
8. Landauer, R., *J. Appl. Phys.*, **23**, 779 (1952).
9. Maxwell, J. C., "A Treatise On Electricity And Magnetism," 3rd edit., Vol. I, Chapt. 9, Art. 314, Dover, New York (1954).
10. Dul'nev, G. N., *Inz-Fiz. Zh.*, **9**, (3), 399 (1965).
11. Baxley, A. L., N. C. Nahas, and J. R. Couper, in "Proceedings of The Seventh Conference on Thermal Conductivity," Natl. Bur. Standards Special Publ. No. 302, 685-694 (Sept. 1968).
12. Tsao, G. T., *Ind. Eng. Chem.*, **53**, (5), 395 (1961).
13. Warren, J. E., and J. H. Messmer, *Ind. Eng. Chem. Fundamentals*, **1** (3), 222,223 (1962).
14. Nielson, L. E., *J. Composite Materials*, **1** (2), 100 (1967).
15. Hamilton, R. L., and O. K. Crosser, *Ind. Eng. Chem. Fundamentals*, **1** (3), 187 (1962).
16. Springer, G. S., and S. W. Tsai, *J. Composite Materials*, **1** (2), 166 (1967).
17. Thornburgh, J. D., and C. D. Pears, *A.S.M.E. Publ. 65-WA/HT-4*, (1965).
18. Jefferson, T. B., O. W. Witzell, and W. L. Sibbitt, *Ind. Eng. Chem.*, **50** (10), 1589-1592 (1958).
19. Jakob, M., "Heat Transfer," Vol. I, p. 88, Wiley, New York (1950).
20. Arpaci, V., "Conduction Heat Transfer," p. 284, Addison-Wesley, Reading, Mass. (1966).
21. Fidelle, T. P., Ph.D. dissertation, Univ. Massachusetts, Amherst (1969).
22. Baxley, A. L., and J. R. Couper, *Univ. Arkansas Eng. Exp. Sta. Res. Rept. No. 8* (1966).
23. Goldsmith, A., et al., "Handbook of Thermophysical Properties of Solid Materials," Macmillan, New York (1961).

Manuscript received June 17, 1970; revision received February 9, 1971; paper accepted February 10, 1971.

Experimental Evaluation of Dynamic Models for a Fixed-Bed Catalytic Reactor

J. A. HOIBERG, B. C. LYCHE, and A. S. FOSS

Department of Chemical Engineering

University of California, Berkeley, California

Experimental observations of a reactor's frequency response when compared with mathematical models of the reactor revealed the need for accurate modeling of heat generation, heat exchange, and heat storage processes. The experiments were performed in a laboratory reactor with the exothermic reaction between hydrogen and oxygen catalyzed by platinum on granules of silica gel. This system permitted observation of several nonlinear effects.

One- and two-dimensional, locally linear, plug-flow models of the continuum type were used for the comparison. One of the models included the effects of intraparticle diffusion of reactants. However, models that neglected intraparticle dynamic effects were found suitable here because the decay time for the diffusion process within the catalyst was short compared to the reactor's major thermal time constant. A two-dimensional model was found to give an excellent representation of the very complex movement of concentration and temperature waves in this type of reactor, while a one-dimensional model was found to serve well when radial gradients are small.

Although many different types of mathematical models of fixed-bed reactors have been in use for several decades, there still remain a number of uncertainties regarding the amount of detail needed in models of the dynamic behavior of these reactors. The catalytic fixed-bed reactor with gaseous reactants, the type of system treated here, is particularly rich in these uncertainties. For example, the generation, transport, and storage of heat are processes of prime importance in this type of reactor, but the detail with which these processes must be represented in dynamic models is not at all certain, and indeed varies from case to case. The misjudgment of this detail may lead, on the one hand, to a model incapable of representing the principal behavior and, on the other, to a model that is computationally and analytically intractable.

These concerns have prompted this experimental investigation of the importance and influence of the numerous physical and physicochemical phenomena active under dynamic conditions. A fixed-bed reactor in which the highly exothermic reaction between hydrogen and oxygen occurred on a platinum catalyst was subjected to sinusoidal disturbances in the feed temperature and feed composition. Shown here is a comparison of the intricate behavior of the resulting temperature and concentration

J. A. Hoiberg is at Continental Oil Company, Ponca City, Oklahoma 74601. B. C. Lyche is with Dow Chemical Company, Terneuzen, The Netherlands.

waves with predictions of various mathematical models of the reactor. The models comprised both one- and two-dimensional continuum representations. Several studies of a similar nature have been reported for liquid reactants (*17* to *19*), but an experimental study of the dynamics of a nonisothermal, catalytic reactor with gaseous reactants seems to have been the subject of only one prior investigation (*6*). Numerous experimental studies have been made under isothermal conditions, but these are of little relevance here because the presence of a temperature wave has profound influence on reactor behavior.

The phenomena whose influence it was possible to investigate via this technique and this reaction system included the dispersive effects of heat transfer process within the bed, temperature-induced variations in fluid linear velocity, and the nature of nonlinear effects. While the importance of heat transfer processes is well appreciated, nonetheless there were questions concerning the relative importance of the heat exchange with the catalyst, the radial transport through the bed, and the exchange with the wall of the reactor. The coupling between linear velocity and the temperature and concentration waves obtains owing to the influence of temperature on gas density and the change in mole number through reaction. Although this coupling may be a source of nonlinear behavior, the major nonlinear effects likely stem from the rate of chemical reaction.

Several effects often of importance under industrial conditions were investigated by computation. Among the most important are diffusional resistance to reactant transport within the catalyst and severe radial temperature gradients. The former may add a further dynamic element to the process and hence complicate the propagation of disturbances. Concern for the latter centers on effective methods for modeling the dynamic response of the reactor under these conditions.

A principal interest in this work was the evaluation of the suitability of locally linearized models in representing the dynamic behavior of the reactor. Our attention has been directed to locally linear models because the results of these experiments and those of prior investigators (*17* to *19*) show that such models are remarkably descriptive of the major effects. Under the conditions normally encountered in reactors under control, the influence of nonlinear effects on dynamic behavior is thoroughly subordinate to the influence of variation of the reaction rate throughout the bed. Thus when one considers the rather sizable uncertainties in the numerical values of the physical and chemical parameters and the relative simplicity of the linearized models, there is little incentive to refine the descriptive ability of the models by retention of the nonlinear representation. Rather, the use of reactor models in control analyses suggests just the contrary.

EXPERIMENTS

Experiments were performed using the platinum-catalyzed reaction between hydrogen and oxygen because the coupling between temperature and concentration for this reaction system is large [the coupling parameter (*7*) was about 6.2] and because the inherent flexibility of the system permitted operation at easily obtained temperature and pressure levels. Appreciable coupling is important because the unique character of these reactors derives from this source.

Reactor

A thin-wall (1 mm.) glass tube about 1 in. in diameter with sample ports spaced every 2 in. axially was used to hold a packed catalyst section 20-in. long. The reactant mixture consisting of 1 mole % oxygen and 99% hydrogen was raised to a temperature of 100°C. by an electric heater located immediately above the bed, and was fed to the top of the tube. Sinusoids in feed temperature were achieved by variation of the power to this heater, while concentration sinusoids were produced by the variation of the oxygen flow rate into a Venturi device that mixed the two gases prior to their introduction into the heater. The entire reactor tube was surrounded by a silvered and evacuated glass jacket for the purpose of reducing heat loss.

The catalyst consisted of granules of silica gel, 0.5 mm. in characteristic dimension, on which platinum in the amount of 0.0015 wt.% was deposited by a method of Benesi (*3*). The activity of the catalyst was quite stable for the duration of these experiments, and was such that under the conditions of operation conversion was virtually complete in the first 70% of the bed. For the conditions of these experiments the catalyst effectiveness factor was believed to range between unity and 0.5. Further properties of the catalyst are given in Table 1.

Measurements

Under conditions of steady sinusoidal forcing, measurements were made of the gas temperature and concentration every 2 in. along the center line of the catalyst bed. Temperature measurements, which could be resolved to within 0.2°C., were made with thermocouples. The oxygen concentration was determined to within 1×10^{-5} oxygen mole fraction by a continuous paramagnetic oxygen analyzer. This device was fed by a small (1% of main stream) continuous sample stream of gas extracted from the center line of the catalyst bed through small diameter stainless steel tubes. Concentration and temperature measurements were also made at several radial locations in the course of the experiments. The temperature of the feed stream and the flow rates of the individual hydrogen and oxygen streams were continuously recorded and served as a reference for the amplitude and phase of the sinusoids within the bed.

Acquisition of Data

The behavior of the reactor was observed at forcing frequencies of 3.5, 7, 14, and 28 cycles/hr. The response at frequencies below this range was essentially a quasi steady state response; above it the attenuation of the sinusoids in the reactor was so large that reliable measurements could not be made. The amplitude of the forcing concentration sinusoid was typically 0.001 mole fraction, while that of the temperature sinusoid ranged between 1.6 and 7°C. and sometimes as high as 10°C. when nonlinear effects were under study. Typical operating conditions

Table 1. Catalyst Properties

True density (no pores)*	137 lb./cu. ft.
Individual particle density ρ_p*	39 lb./cu.ft.
Bulk density*	24.0 lb./cu.ft.
Surface area (internal)*	340 sq. m./g.
Pore volume*	1.15 cc./g.
Estimated avg. pore radius $\left(2 \times \frac{\text{pore vol.}}{\text{surf. area}}\right)$	68×10^{-8} cm.
Specific heat (25°C.)*	0.22
Thermal conductivity of silica gel	0.08 B.t.u./(hr.)(ft.)(°F.)
Experimentally determined properties	
Void fraction of bed ϵ	0.35
Particle diameter d_p (cut between 28-32 Tyler sieves)	0.5 mm.
Estimated properties	
Mean free molecular path for hydrogen in pores,	15×10^{-6} cm.
Knudsen diffusivity of oxygen	2.2×10^{-2} sq.cm./sec.

* From *Bulletin No. 303*, Davison Chemical Company, Catalyst Grade 59.

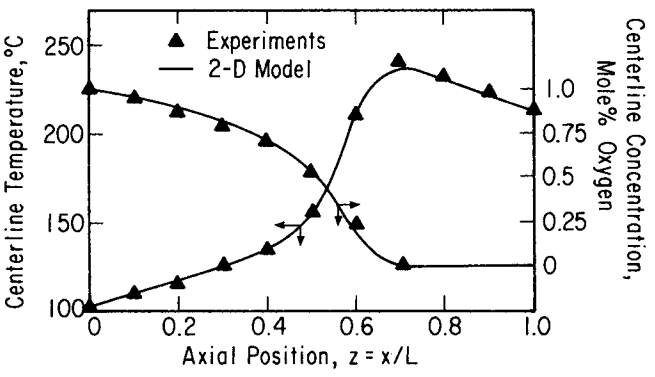

Fig. 1. Typical steady state profiles of temperature and concentration.

TABLE 2. TYPICAL OPERATING CONDITIONS

Inlet oxygen concentration (mole %)	1.0
Inlet hydrogen concentration (mole %)	99.0
Inlet temperature at center line	100°C.
Room temperature	25°C.
Adiabatic temperature rise	167°C.
Actual maximum temperature rise	125°C.
Heat released by complete reaction	7.5 cal./sec.
Heat loss through wall	1.9 cal./sec.
Inlet pressure	20 lb./sq.in.abs.
Pressure drop in bed	2.3 lb./sq.in.
Volumetric feed rate (at 20°C., 1 atm.)	9,400 cc./min.
Inlet empty tube velocity	36 cm./sec.
Nominal gas residence time	0.5 sec.
Inlet mass flux G_0 (based on empty tube area)	23.7 lb./(hr.)(sq.ft.)
Inlet particle Reynolds number, d_pG_0/μ	1.7
Radial gradients	
Inlet	
$(T_{wall} - T_{center})$	−5°C.
$(y_{wall} - y_{center})$	0.0% oxygen
Maximum gradients in bed	
$(T_{wall} - T_{center})$	−11°C.
$(y_{wall} - y_{center})$	0.10% oxygen

for these experiments are given in Table 2, and typical profiles of temperature and concentration at steady state are shown in Figure 1.

Amplitude and phase information was determined from the recorded signals at each sample port. Usually three complete periods were used to determine the temperature data, but only one or two periods of the concentration response was acquired and used owing to the excessive time required to obtain these data with just one analytical instrument.

EXPERIMENTAL RESULTS

Several different types of reactor behavior are presented here for the purpose of displaying some of the more interesting characteristics of fixed beds. In addition to the frequency response behavior, we show the "wrong-way" transient (*4, 8, 7*) resulting from a step change in the temperature of the feed stream and the influence of nonlinearities on the sinusoids when the peak-to-peak excursions of temperature within the bed exceed 100°C.

Confirmation of "Wrong-Way" Behavior

With the reactor operating at steady conditions typical of those given in Table 2, a decrease in the temperature of the reactant feed produces the behavior shown in Figure 2, which at locations in the latter half of the bed appears to have the wrong sense initially. As explained by prior investigators (*8*), this behavior results because the fluid that sweeps through the slowly advancing cold zone has a reactant concentration higher than that at steady state and therefore increases the rate of heat generation in regions of the bed ahead of the thermal wave. However, as Figure 2 shows, the increased rate of heat generation acts to increase temperature only in regions of the bed where the reaction rate is large, which here obtains in the region $0.5 < y < 0.65$. Early in the bed and near the end of the bed where the reaction rate is smaller, the thermal wave behaves much as it would in a nonreactive bed. The appearance of the "wrong-way" temperature transient in some parts of the bed but not in others results from the spatial variation of the competing effects of heat generation and the dispersion of heat through heat transfer processes.

Nonlinear Effects

Distortions in sinusoids that occur when temperature excursions are large may be seen in the facsimile of an experimental record shown in Figure 3. Here the peak-to-peak excursions in temperature reached a maximum of 114°C. at location $z = 0.4$. The concentration waves that obtain under these conditions are nearly mirror images of the temperature waves owing to the strong coupling between these two variables through the reaction rate. Of the several features that may be noticed, the most striking is the superficial simplicity of the distortions. At location $z = 0.4$, the sinusoids are simply sharpened at the crests, flattened at the troughs, and slightly skewed, with the back side of the waves being the steepest. It is likely that

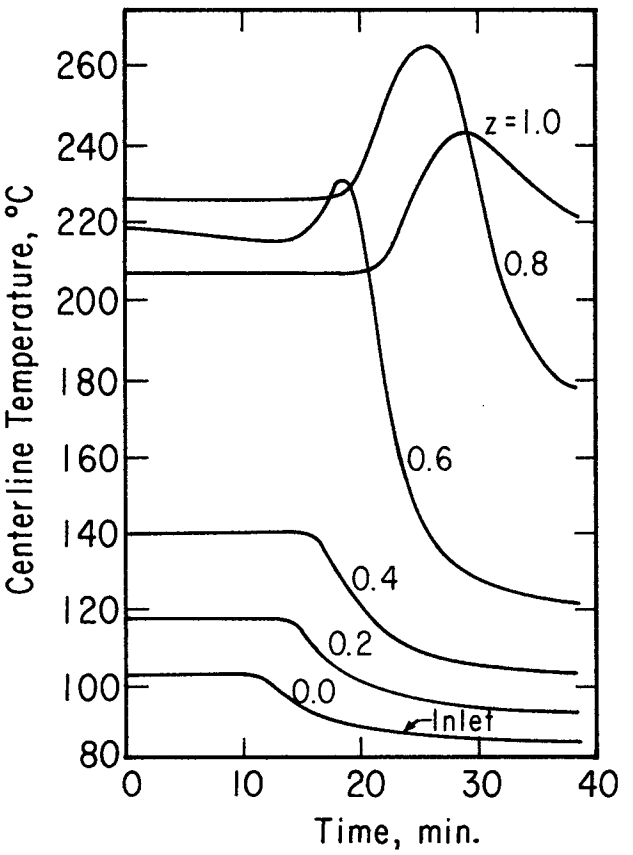

Fig. 2. Experimentally determined temperature transients in response to a decrease in feed temperature.

the sharpened crests and flattened troughs in this region obtain owing to the convexity of the reaction rate dependence on temperature. At location $z = 0.8$, however, the situation is just the reverse; the peaks are flattened and the troughs are sharpened. The flattening of the temperature crests results from the flattening of the troughs of the concentration wave, which occurs in this portion of the reactor owing simply to the near absence of oxygen. While the oxygen concentration was not measured in this particular experiment, such distortions in the oxygen wave were observed in other instances. The cause of the trough sharpening in this region is not known. It is noticed that the back side of the wave in this region is still the steepest; the phenomena contributing to wave steepening were not investigated however.

The behavior shown in Figure 3 may be considered that of the quasi steady state because the frequency was quite low (3.5 cycles/hr.). The nonlinear effects were most prominent under such conditions because of the small attenuation of the thermal waves in the heat exchange process. As the frequency was increased, the amplitude of the waves diminished owing to the influence of heat exchange, and because the nonlinear effects emanate primarily from the temperature dependence of the reaction rate, their influence diminished also. At a frequency of 14 cycles/hr., for example, the attenuation of the thermal waves was so large that no nonlinear effects could be detected. Through a number of experiments of this type, it was found that the nonlinear effects described above had negligible influence when the excursions in temperature everywhere in the reactor were less than 15°C. Our further experiments, which were used to evaluate locally linear models of the reactor, were conducted such that this condition was satisfied.

Frequency Response

We present here the experimentally determined behavior of the temperature and concentration waves as they progress through the bed. In the presentation employed here, the amplitude and phase of a wave of a given frequency are displayed as a function of distance along the bed. These wave profiles are shown for a number of frequencies over the range in which dynamic effects were measurable. This method of presentation, which differs from the usual, has the distinct advantage that it allows display of the sometimes intricate evolution of the waves.

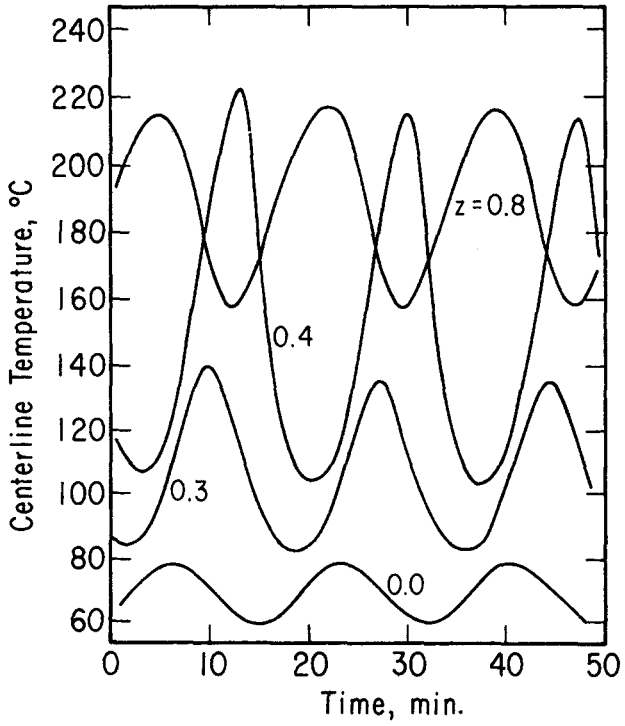

Fig. 3. Experimentally determined response to sinusoidal temperature forcing of large amplitude.

The conditions under which these experiments were conducted were nominally those stated in Table 2, but, in fact, the conditions for each run differed slightly from these owing to the impossibility of attaining identical steady state conditions for all runs. These differences were accounted for in the calculations described later and therefore presented no complication in the evaluation of mathematical models.

The experimental results are shown in Figures 4, 5, and 6. Shown here also by the continuous cures are the results of calculations based on a two-dimensional model that is described in a later section. Also deferred until later are the implications of the correspondence between the experimental and calculated results. All results in these figures pertain to the center line of the bed.

These graphs convey at a glance the complex nature of the propagation of temperature and concentration disturbances through the reactor. The interpretation of these complexities is lengthy and is not presented here because the interpretations given in an earlier paper (*18*) apply here as well. It should suffice at this point to make the following observations:

Temperature Forcing (Figure 4)

1. Both the temperature and concentration waves are strongly influenced by frequency, which implies that heat generation by reaction competes with attenuation of the waves due to heat exchange processes.
2. The dominance of the temperature wave everywhere in the bed is revealed by the similarity of the concentration and temperature amplitudes in the latter part of the bed, by the similarity of the temperature phase to that observed in an unreactive bed, and the abrupt adjustments of about 180 deg. in the concentration phase in regions where concentration and temperature phase become nearly equal (*18*).
3. Except for regions of rapid chemical reaction, the agreement between experiment and calculated results is remarkably good.

Concentration Forcing (Figures 5 and 6)

1. The concentration wave is clearly dominant in the early portion of the bed as indicated by the small phase angles of both waves and the phase relation between them.
2. Neither wave appears to dominate in the more reactive part of the bed except at the lowest frequency (3.5 cycles/hr.) where the sharp spike in amplitudes and the phase relationships imply that the temperature wave is dominant.
3. The curious phase lead in the concentration wave that was observed earlier by calculation (*18*) is here observed experimentally. An explanation of this behavior is contained in the earlier paper.
4. With the exception of the phase of the temperature wave at high frequency, the correspondence between calculations and experiment is good here also.

Measurements were also made of the wave behavior across the radius of the reactor, and the results revealed nothing extraordinary. For example, the amplitude of the temperature wave under temperature forcing decreased across the radius much as would be found in an unreactive bed; the presence of heat generation, except in the

most reactive zone, had very little influence. Some detailed results are reported in reference *10*.

MATHEMATICAL MODEL

The mathematical model employed here is a continuum, two-dimensional representation similar to the models of many earlier investigators. Incorporated in the model is the phenomenon of temperature-induced velocity variations; a radial profile in velocity is also acknowledged. No axial fluid mixing or axial diffusion is included because such sources of axial dispersion are known to be small compared to dispersion resulting from coupling between waves of differing propagation speeds and that resulting from heat exchange processes (*8*). The temperature throughout each catalyst particle is taken to be uniform because an analysis showed the temperature to be virtually uniform owing to the high thermal diffusivity. While it is not so definite that reactant concentration within the catalyst is uniform, it is nevertheless assumed uniform in the model under discussion here. Another model considered later in the paper treats concentration gradients within the catalyst. The influence of the reaction product, water in this case, was found to be negligible in all respects and therefore is not included in the model. With the exception of the reaction rate parameters, all other parameters were considered constant even though some variation was experienced; the influence of these variations was second order. The treatment of the kinetic parameters is discussed shortly.

Primitive Equations

Total mass balance

$$\frac{\partial \rho_f}{\partial t} + \frac{\partial (\rho_f v_f)}{\partial x} = 0 \qquad (1)$$

B.C.: $\rho_f(t, 0, r) = \rho_f^0(t)$
$v_f(t, 0, r) = v_f^0(t, r)$

Mass balance for limiting reactant (oxygen) in fluid

$$[\epsilon + (1 - \epsilon)\epsilon_p] \frac{\partial (\rho_f w)}{\partial t} + \epsilon \frac{\partial (\rho_f v_f w)}{\partial x} + \frac{1}{r} \frac{\partial}{\partial r} (r q_m) = - M R^* \qquad (2)$$

where

$$R^* = k p^n \exp \{- E/R_g T_p^*\} \qquad (3)$$

$$q_m = - \rho_f D_b \frac{\partial w}{\partial r}$$

B.C.: $w(t, 0, r) = w^0(t, r)$

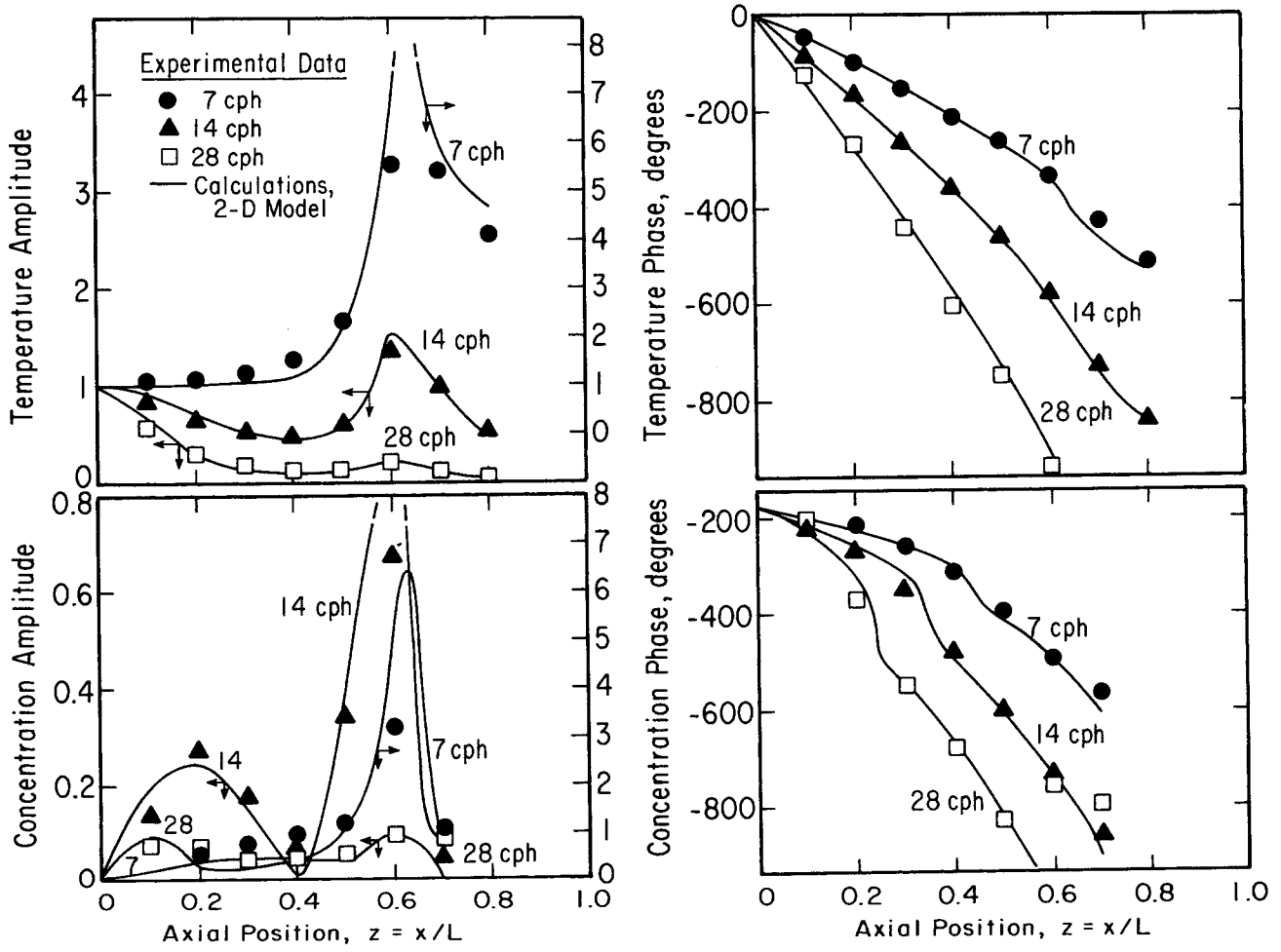

Fig. 4. Amplitude and phase behavior of temperature and concentration waves at the center line: temperature forcing.

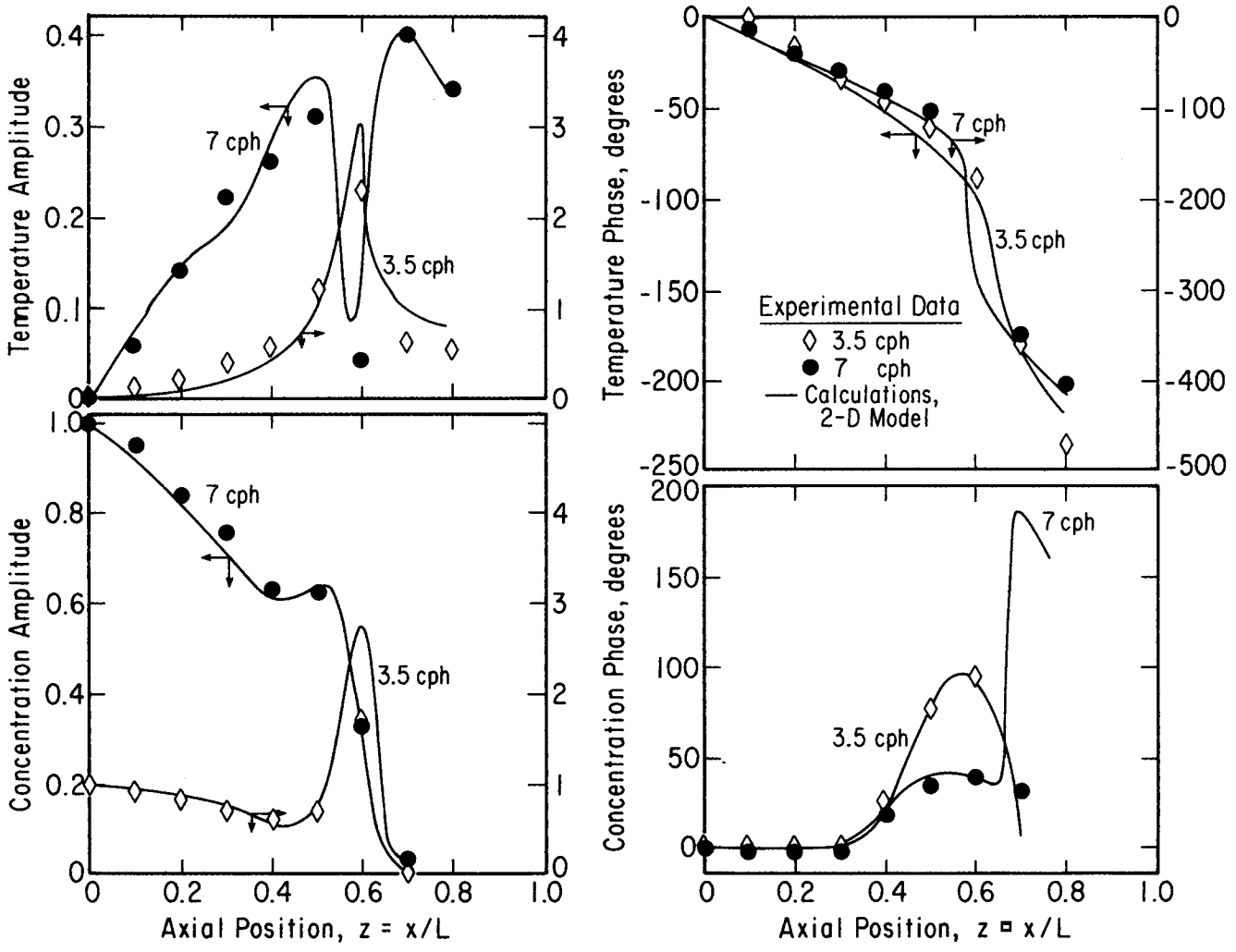

Fig. 5. Amplitude and phase behavior of temperature and concentration waves at the center line: low frequency concentration forcing.

$$\left.\frac{\partial w}{\partial r}\right|_0 = \left.\frac{\partial w}{\partial r}\right|_{R_1} = 0$$

Heat balance for fluid

$$\epsilon c_f \frac{\partial(\rho_f T_f^*)}{\partial t} + \epsilon c_f \frac{\partial(\rho_f v_f T_f^*)}{\partial x} + \frac{1}{r}\frac{\partial}{\partial r}(r q_h) = h_p a (T_p^* - T_f^*) \quad (4)$$

where

$$q_h = -k_e \frac{\partial T_f^*}{\partial r}$$

B.C.: $T_f^*(t, 0, r) = T_f^{*0}(t, r)$

$$\left.\frac{\partial T_f^*}{\partial r}\right|_0 = 0$$

$$\left.k_e \frac{\partial T_f^*}{\partial r}\right|_{R_1} = -h_w(T_f^*|_{R_1} - T_w^*) \quad (5)$$

Blake-Kozeny relation for the pressure gradient

$$\frac{\partial P_T}{\partial x} = -k_b \mu_f v_x \quad (6)$$

B.C.: $P_T(t, 0, r) = P_T^0$

Radial profile of fluid velocity (assumed similar)

$$v_f(t, x, r) = v_x(x, t) \cdot v_r(r) \quad (7)$$

with the normalization

$$\frac{2}{R_1^2}\int_0^{R_1} r v_r dr = 1$$

The specification of the function v_r is described later.

Equation of state (ideal gas law)

$$\rho_f = \frac{M_f P_T}{R_g T_f^*} \quad (8)$$

Heat balance for a catalyst particle

$$(1-\epsilon)\rho_p c_p \frac{\partial T_p^*}{\partial t} = h_p a (T_f^* - T_p^*) + (-\Delta H) R^* \quad (9)$$

Heat balance for the tube wall

$$\rho_w c_w (R_2^2 - R_1^2)\frac{\partial T_w^*}{\partial t} = 2 h_w R_1 (T_f^*|_{R_1} - T_w^*) + 2U^* R_2 (T_e^* - T_w^*) \quad (10)$$

Implicit in these equations are a number of assumptions not previously stated. There is assumed to be no resistance to the transfer of reactants from the fluid to the catalyst; a resistance to the transfer of heat, however, is known to be significant in general and is therefore included. Models of a similar nature have been considered by Carberry and White (5). Also incorporated is a resistance to the transfer of heat between the fluid and the tube wall. In determining reactor pressure excursions, fluid inertia is neglected because the transients are slow.

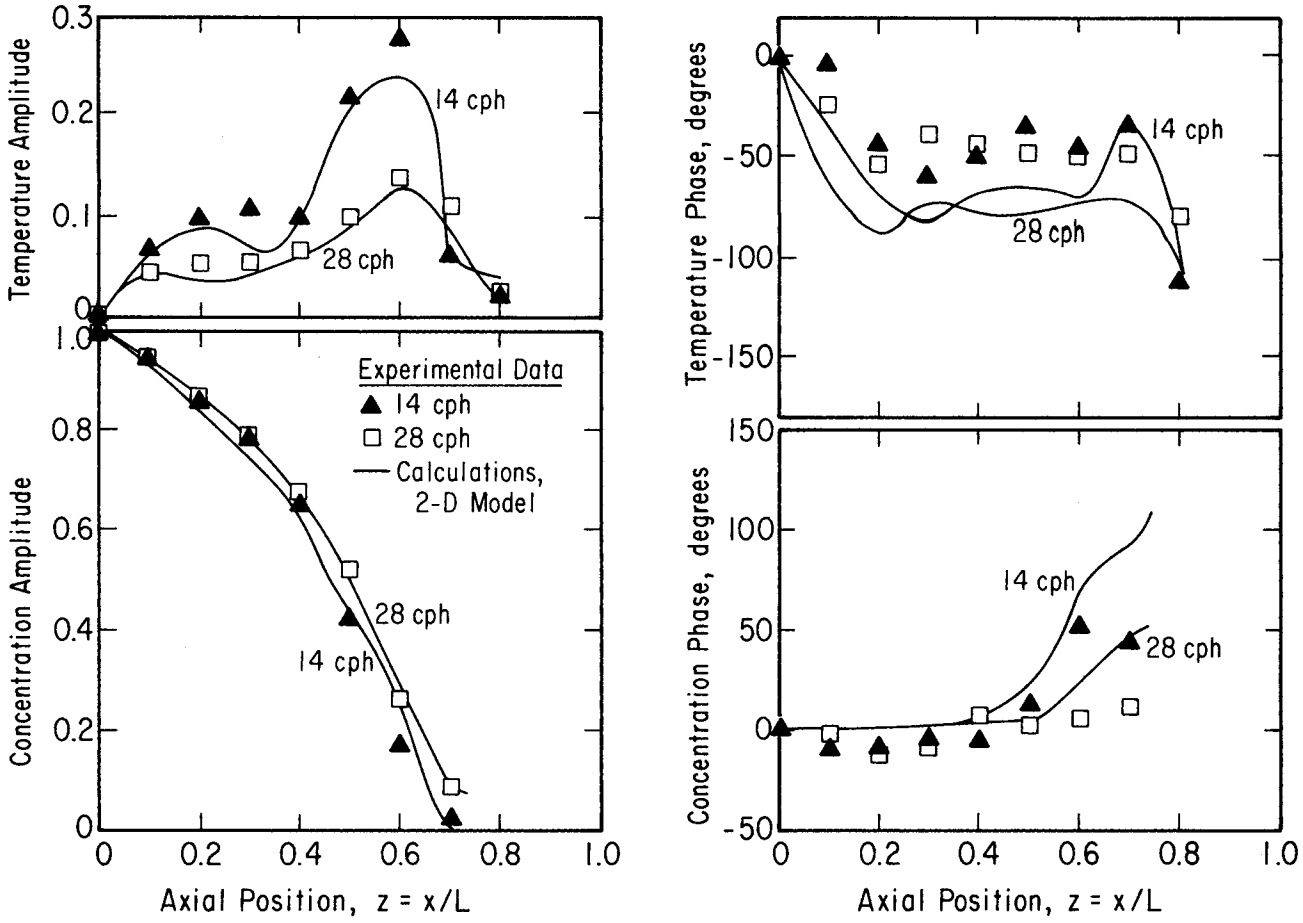

Fig. 6. Amplitude and phase behavior of temperature and concentration waves at the center line: high frequency concentration forcing.

Normalization and Linear Approximation

In the development of a model suitable for small excursions of the variables about their steady state values, the nonlinear terms in the above equations are expanded in a Taylor series and only the first-order terms retained. The results of this operation are presented here in terms of variables representing deviations from the local steady state and normalized with respect to the steady state values of the variable at the bed entrance. Temperature, however, is normalized with respect to the adiabatic temperature rise. Furthermore, because the molecular weight of the fluid is essentially constant, it is convenient to express the oxygen concentration in terms of mole fraction. The oxygen partial pressure may be expressed as the product of the total pressure and the mole fraction because the gas is essentially ideal. Finally, time is normalized by the nominal residence time, axial distance by the total bed length, and radial distance by the tube radius.

With these normalizations, the equations for the locally linear model are

Total mass balance

$$\frac{\partial(\delta\rho)}{\partial\tau} + \frac{\partial(\rho_s\delta v)}{\partial z} + \frac{\partial(v_s\delta\rho)}{\partial z} = 0 \qquad (11)$$

$$\delta\rho(\tau, 0) = \delta\rho^0, \delta v(\tau, 0, \mathrm{r}) = \delta v^0(\tau, \mathrm{r})$$

Oxygen mass balance

$$\left\{1 + (1-\epsilon)\frac{\epsilon_p}{\epsilon}\right\}\rho_s\frac{\partial(\delta Y)}{\partial\tau} + (1-\epsilon)\frac{\epsilon_p}{\epsilon}Y_s\frac{\partial(\delta\rho)}{\delta\tau} + v_r\frac{\partial(\delta Y)}{\partial z} + (\rho_s\delta v + v_s\delta\rho)\frac{\partial Y_s}{\partial z} - \frac{1}{Pe_m}\frac{1}{\mathrm{r}}\frac{\partial}{\partial\mathrm{r}}\left(\mathrm{r}\frac{\partial(\delta Y)}{\partial\mathrm{r}}\right) = -R_p\delta P - R_Y\delta Y - R_T\delta T_p \qquad (12)$$

$$\delta Y(\tau, 0, \mathrm{r}) = \delta Y^0(\tau, \mathrm{r}); \quad \left.\frac{\partial(\delta Y)}{\partial\mathrm{r}}\right|_0 = \left.\frac{\partial(\delta Y)}{\partial\mathrm{r}}\right|_1 = 0$$

where

$$\left.\begin{aligned} R_P &\equiv \frac{\partial R_s}{\partial P_s} = \frac{nR_s}{P_s} \\ R_Y &\equiv \frac{\partial R_s}{\partial Y_s} = \frac{nR_s}{Y_s} \\ R_T &\equiv \frac{\partial R_s}{\partial T_{ps}} = \frac{AT_0}{(T_0 + T_{ps})^2}R_s \\ R_s &\equiv KP^nY^n\exp\left\{\frac{AT_{ps}}{T_0 + T_{ps}}\right\} \end{aligned}\right\} \qquad (13)$$

Heat balance for fluid

$$\rho_s\frac{\partial(\delta T_f)}{\partial\tau} + v_r\frac{\partial(\delta T_f)}{\partial z} + (\rho_s\delta v + v_s\delta\rho)\frac{\partial T_{fs}}{\partial z} - \frac{1}{Pe_h}\frac{1}{\mathrm{r}}\frac{\partial}{\partial\mathrm{r}}\left(\mathrm{r}\frac{\partial(\delta T_f)}{\partial\mathrm{r}}\right) = H(\delta T_p - \delta T_f) \qquad (14)$$

$$\delta T_f(\tau, 0, \mathrm{r}) = \delta T_f{}^0(\tau, \mathrm{r})$$

$$\left.\frac{\partial(\delta T_f)}{\partial\mathrm{r}}\right|_0 = 0$$

$$\left.\frac{\partial(\delta T_f)}{\partial\mathrm{r}}\right|_1 = Nu(\delta T_w - \delta T_f|_1)$$

Pressure drop

$$\frac{\partial(\delta P)}{\partial z} = -K_b(\mu_s \delta v_z + v_{sz}\delta\mu) \tag{15}$$

$$\delta P(\tau, 0, \mathrm{r}) = \delta P^0(\tau)$$

Velocity profile

$$\delta v = v_r \cdot \delta v_z \tag{16}$$

Equation of state

$$\delta\rho = \frac{T_0}{T_0 + T_{fs}}\delta P - \frac{T_0 P_s}{(T_0 + T_{fs})^2}\delta T_f \tag{17}$$

Heat balance for catalyst

$$\frac{\partial(\delta T_p)}{\partial\tau} = H\beta(\delta T_f - \delta T_p) + \beta(R_P\delta P + R_Y\delta Y + R_T\delta T_p) \tag{18}$$

Heat balance for tube wall

$$\frac{\partial(\delta T_w)}{\partial\tau} = H_w\beta_w(\delta T_f|_1 - \delta T_w) - U\beta_w\delta T_w \tag{19}$$

The steady state distributions of fluid temperature T_{fs}, concentration Y_s, and so on, needed for the solution of these equations are obtained from the normalized primitive equations with all derivatives with respect to time set identically zero.

Several further approximations could be made under the conditions of these experiments. Because the accumulation of total mass, oxygen, and fluid enthalpy were so small, terms involving derivatives with respect to time in Equations (11), (12), and (14) were dropped from the model. Temporal changes in gas viscosity were also disregarded. Finally, all steady state calculations were made with $T_{ps} = T_{fs}$ because the difference in catalyst and fluid temperature was less than 2°C. It is noticed, however, that the fluid and catalyst temperatures are considered different in the dynamic model [Equations (14) and (18)] so that the dispersion due to heat exchange is included.

The frequency response is most easily calculated by application of the Laplace transformation to the linearized equations and by replacement of the complex variable of the transformation by the pure imaginary number $j\omega$. In this procedure, all initial conditions are taken zero. The integration was performed numerically using a version of the Crank-Nicolson method similar to that suggested by von Rosenberg (*20*). Step sizes of $\Delta z = 0.02$ and $\Delta r = 0.1$ were used.

The boundary conditions at the reactor inlet used in these calculations required considerable attention, because under the conditions of the experiment they were not simple. For example, because of heat loss from the gas prior to its entrance into the catalyst bed, radial temperature profiles at the bed entrance were appreciable and had to be specified for both the steady state fluid temperature T^0_{fs} and the temperature deviation $\delta T_f{}^0$. The profile of the steady state temperature was approximated as follows from experimental measurements of temperatures at the center line, near the wall, and of the surroundings:

$$T_{fs}{}^0(\mathrm{r}) = T_{fs}{}^0(0) + A\mathrm{r}^2 + B\mathrm{r}^4$$

where

$$A = 2\,[T_{fs}{}^0(1) - T_{fs}{}^0(0)] + \frac{\gamma}{2}\,[T_{fs}{}^0(1) - T_e]$$

$$B = T_{fs}{}^0(1) - T_{fs}{}^0(0) - A$$

$$\gamma = Nu \cdot U/(H_w + U)$$

It is noticed that this form assures continuity of the wall heat flux at the bed entrance. The boundary condition for the temperature deviation variable was approximated from experimental measurements of the amplitude and phase relationships across the radius at the bed entrance. The actual function used to approximate the complex-valued deviation variable at the bed entrance was the zero-order Bessel function $J_0(\lambda r)$, with λ a complex variable chosen such that the experimentally determined amplitude and phase at the wall ($r = 1$) relative to the sinusoid at the center line were given by $J_0(\lambda)$. This form of radial profile was chosen because it is the form of the frequency response function for the temperature of a fluid in rodlike flow in a long tube (*10*). This same form was taken for small radial concentration variations that were observed inexplicably in the reactant feed at the high frequency forcing of feed temperature. Slight fluctuations in the mass feed rate of reactants were noted during temperature forcing, but their influence on the calculated results was negligible and were therefore disregarded. For the forcing of feed concentration, it was experimentally verified that the oxygen concentration across the radius was uniform, and hence the boundary conditions for this case were simple. Deviations in fluid velocity and density at the inlet were both taken zero.

Evaluation of Parameters

Numerical values of nine of the twelve parameters of the model were determined from a series of independent experiments. Typical values of all 12 parameters are given in Table 3. Of these, the most critical to the accuracy of the model are the reaction rate parameters K and $A = E/R_gT_i{}^\circ$, and because of their dependence on the state of the catalyst, values of these two parameters were determined for the specific operating conditions of each dynamical experiment. The values of the remaining parameters with the exception of the Peclet number for mass transport were determined only once during the course of these experiments.

The sequence of experiments from which the parameters were determined began with:

1. Nonreactive bed at steady state

The outside heat transfer parameter U could be determined directly from the measured temperature change along the center line without knowledge of the bed thermal resistance or other thermal resistances because the outside resistances dominated entirely. The coefficient K_b in the Blake-Kozeny relation was similarly determined in a steady state experiment through measurement of the pressure profile. A least-squares criterion was used in both determinations.

2. Frequency response of nonreactive bed

Experimental amplitude and phase information at five frequencies, when fitted in the least-squares sense to the predictions of the two-dimensional model, gave values for the thermal Peclet number Pe_h and the heat transfer parameters H and H_w. These determinations, which are similar to those of Ball (*2*), made use of both axial and radial information.

3. "Differential" reactor

Measurements of small changes in temperature and oxygen concentration across a thin (3 to 5 mm.) bed of catalyst revealed that the apparent activation energy of the reaction first increased with temperature and then decreased for temperatures above 210°C. (*10*). These observations suggested that parameters K and A be taken as functions of axial location, and in this work the functions

TABLE 3. TYPICAL VALUES OF DIMENSIONLESS PARAMETERS (AND THE CORRESPONDING DIMENSIONAL PARAMETERS) FOR THE TWO DIMENSIONAL MODEL

Dimensionless parameters	Typical values	Dimensional parameters*	Corresponding values
β	1.3×10^{-3}	c_f	3.0 pcu/(lb.)(°C.)
		c_p	0.204 pcu/(lb.)(°C.)
β_w	1.3×10^{-3}	c_w	0.204 pcu/(lb.)(°C.)
		ρ_w	139 lb./cu.ft.
T_0	2.25	T_i*	376°K.
		$(-\Delta H)$	1.162×10^{-5} pcu/lb.-mole O_2
		M_f	2.3 lb./lb.-mole
A	16	E	12,000 cal./g.-mole
K	0.875	k	$3.86 \times 10^4 \frac{\text{lb.-mole } O_2}{(\text{psfa } O_2)^{0.8}\,(\text{hr.})\,(\text{cu.ft.})}$
n	0.8	——	——
K_b	0.079	$\frac{k_b}{\mu_{fi}}$	1.77×10^8 ft.$^{-2}$
			6.44×10^{-11} (lb.$_f$)(hr.)/sq.ft.
H	400	h_p	8 pcu/(hr.)(sq.ft.)(°C.)
		a (spherical particles assumed)	2,400 ft.$^{-1}$
H_w	66	h_w	60 pcu/(hr.)(sq.ft.)(°C.)
U	0.48	U*	0.4 pcu/(hr.)(sq.ft.)(°C.)
Pe_h	0.48	k_e	0.14 pcu/(hr.)(ft.)(°C.)
Pe_m	4.7	D_b	0.775 sq.ft./hr.

* These parameters, with those given in Tables 1 and 2, provide a complete set for specification of the two-dimensional model.

were simple: Two different sets of values of K and A were used, one for high temperature regions and one for low temperature regions. Also by the use of the differential reactor, the value of the concentration exponent n was found to be 0.8, in agreement with prior investigators (*14, 15*).

4. Reactor at steady state

The kinetic parameters K and A were determined such that the calculated temperatures at the center line of the reactor matched the measured temperatures in the least-squares sense. The efficacy of this technique may be judged from the representation of the experimental data by the model as shown in Figure 1. As mentioned above, two sets of values of K and A were used in this procedure. Used in these calculations was a Peclet number for radial mass transport that was determined from comparison of measured and calculated radial profiles of oxygen concentration. An accurate value of the mass Peclet number could not be determined from these experiments nor was it needed because the model was quite insensitive to the value of this parameter. Prior investigators (*5*) have made a similar observation.

To complete the model, the radial velocity function v_r must be specified. A profile having a sharp peak about 15% greater than the mean fluid velocity and situated close to the wall was used in some of our calculations. This form is suggested by the experimental observations of Schwartz and Smith (*16*). However for the calculations reported in Figures 4, 5, and 6 the velocity profile was assumed to be flat.

IMPLICATIONS OF EXPERIMENTAL AND CALCULATED RESULTS

These experiments and calculations lead to several conclusions concerning the importance of physical and chemical phenomena under dynamic conditions.

Nonlinear Effects

Nonlinear behavior appears to be quasi-statically related to the effect of temperature and concentration on the rate of chemical reaction. There is little evidence in the experimental results that significant nonlinearities develop owing to dynamic factors. For example. the variation of gas density may, in principle, lead to the steepening or flattening of temperature wave fronts, but there is only very slight evidence of such behavior in our results. The coupling of the temperature and concentration variables with the fluid-flow variables is thus inferred to be of little consequence.

Velocity Profile

It appears that the radial profile of gas velocity is also of little consequence. This conclusion derives from calculations of the model made with an arbitrarily specified profile that possessed a peak near the wall about 15% higher than the mean velocity. Steady state and frequency response results for this case, compared with those for a uniform velocity profile, were found virtually identical to the latter. This seems to imply that the radial transport of heat and matter is rapid enough to counteract the effects of a higher velocity near the wall. The presence of a velocity profile may, however, contribute to the axial dispersion of heat and matter by a process similar to Taylor dispersion, but the magnitude of such an effect is not known. Because of influence of a radial profile in velocity seemed secondary in all respects in these experiments, all calculations were conducted with a uniform profile.

Heat Transfer Processes

Perhaps the most important physical process influencing the dynamic behavior of reactors of small diameter is the radial flow of heat through the bed into the tube wall. In the present case the thermal capacitance of the wall was approximately that of the catalyst, and the thermal resistance of the bed was by far the largest of all resistances, except the resistance exterior to the tube. The rate of heat

exchange between fluid and catalyst was high and therefore contributed only slightly to the axial dispersion of heat. The bulk of the axial dispersion of heat under dynamic conditions, therefore, is attributable to the finite rate of heat exchange between the bed and the tube wall. It is noticed that this heat exchange process remains dominant even when the reactor tube is perfectly thermally insulated from the surroundings.

Intraparticle Effects

There were indications that some diffusional resistance to reactant transport was present in the catalyst in the high temperature regions of the reactor. The resistance to the flow of heat, however, was negligible. The maximum temperature difference within the catalyst was estimated to be about 0.01°C. Estimates of the catalyst effectiveness factor in the high temperature regions using experimentally determined reaction rates and an effective diffusivity equal to 1/20 of the Knudson diffusivity given in Table 1 indicated that the effectiveness factor was about 0.5. Furthermore, the temperature dependence of reaction rates measured with a differential reactor suggested a diffusion influence at high temperatures (>210°C.) (*10*). It is not at all certain, however, that these two observations necessarily imply the existence of an appreciable diffusional resistance; too many facts remain unknown. There is the possibility, for example, that in a catalyst as dilute as that used here, the platinum crystals are not uniformlly distributed throughout the particle, but rather concentrated near the exterior surface. Should this be the case, catalyst effectiveness factors calculated assuming uniformity would be in error.

Nonetheless, it was of interest to us to calculate the dynamic behavior of reactant concentration in a uniformly impregnated catalyst particle and to determine the influence that intraparticle diffusion resistance would exert on reactor behavior under the conditions of these experiments. For the purpose of determining the principal effects, it is sufficient to consider the reaction to be first order and the particles spherical. Then, the mass balance for the limiting reactant in the catalyst pores has the form

$$\frac{\partial^2\eta}{\partial\xi^2} + \frac{2}{\xi}\frac{\partial\eta}{\partial\xi} - \phi\frac{\partial\eta}{\partial\tau} = K(z)f(T_p)\cdot\eta \qquad (20)$$

with boundary conditions

$$\eta(0,\tau) = Y(\tau)$$
$$\left.\frac{\partial\eta}{\partial\xi}\right|_0 = 0$$

The dynamic behavior of the catalyst particle is perhaps most conveniently observed through its frequency response, which is readily obtained from Equation (20) upon linearization of the reaction rate term $f(T_p)\eta$. The result is

$$\delta\eta(j\omega,\xi) = \frac{\sinh\alpha_1\xi}{\xi\sinh\alpha_1}\delta Y(j\omega) + \frac{K_c f_s' Y_s}{\phi\omega j}\left[\frac{\sinh\alpha_1\xi}{\xi\sinh\alpha_1} - \frac{\sinh\alpha\xi}{\xi\sinh\alpha}\right]\delta T_p(j\omega) \qquad (21)$$

where

$$\alpha^2 = r_\eta = K_c(z)f(T_p)$$
$$\alpha_1^2 = r_\eta + \phi\omega j$$

The range of the numerical values of α and α_1 is important. Under the conditions of these experiments, the frequency $\phi\omega$ was less than 0.02 and r_η ranged between 1 at the inlet and 60 at the most reactive point in the bed. Thus since the imaginary part of α_1 is small relative to the real part, it is readily concluded from Equation (21) that the concentration of reactant within the catalyst is independent of the forcing frequency throughout the entire bed. Thus, for the conditions of these experiments, resistance to mass transport within the catalyst does not add a further dynamic element to the process; rather, the retardation of the reaction rate can be treated as a strictly quasistatic effect. Therefore if the formulation of the dynamic model given in Equations (1) to (10) is to be retained, one may incorporate the influence of diffusional resistance simply by allowing the parameters k and E of the rate expression [Equation (3)] to be functions of position in the reactor.

The influence of intraparticle diffusional resistance on the reactor's frequency response was calculated using Equation (21) in the determination of the reaction rate. The major effect of intraparticle resistance was manifest as a dimunition of the large peaks in temperature and concentration amplitude that occur at position $Z = 0.6$ (cf. Figures 4 to 6), which is in accord with a trend that can be noticed in the experimental results. This dimuition may be attributed to changes in the steady state sensitivity functions, which in this model are the counterparts of the functions R_y and R_T. While these effects may be accounted for by Equation (21), such complexity may not always be necessary. Perhaps the simplest way of accounting for them is the use of multilevel choices for the kinetic parameters K and A. Although our observations suggest a choice of three levels (one each for the low and intermediate temperatures and a third for the high temperature region in which diffusional resistance appears influential), only two levels of parameters were used. In the two-dimensional model, the two levels pertained to the low and intermediate temperatures, and no account was taken of the apparent decrease in actviation energy in the region of highest temperature.

The adsorption and transport of water (the product of reaction) within the catalyst were determined by calculation to have negligible effect on reactor behavior, because at the temperature levels of these experiments (100° to 240°C.) the adsorbed water level was very low. At lower temperatures, however (say near room temperature), the influence is pronounced because the thermal effects accompanying the adsorption-desorption process all but dominate the thermal dynamics of the reactor (*12, 13*).

In the study of the intraparticle effects discussed above, there was no need to consider two-dimensional effects in the bed. To simplify the calculations therefore, use was made of the one-dimensional model given in the Appendix. Although not shown here, the transport of water within the catalyst was treated similar to that of oxygen transport and a well-established equilibrium relationship (*11*) was used for the catalyst water content. Adsorbed water was assumed to have no influence on the reaction rate (*14*).

A ONE-DIMENSIONAL MODEL

There are numerous incentives to consider a one-dimensional dynamic model for the reactor. In the present case, the small radial tempearture differences relative to the absolute temperature level naturally suggests such an attempt. Furthermore, there are instances in which models more detailed than a one-dimensional model cannot be justified in view of the uncertainties in reaction stoichiometry and values of the kinetic and heat transport parameters. Also, analyses of reactor control problems are more easily accomplished with one-dimensional models. Pre-

sented here is such a model that may find use in these circumstances.

As suggested by the results of the experiments and calculations discussed above, it is assumed in the formulation of the one-dimensional model that there is no pressure drop and that velocity and density fluctuations are negligible. To further simplify the model, the exponent n in the rate expression is taken to be unity instead of 0.8. Then the following locally linearized equations follow from those given earlier:

Oxygen mass balance

$$\left(1 + (1-\epsilon)\frac{\epsilon_p}{\epsilon}\right)\frac{\partial(\delta Y)}{\partial\tau} + \frac{\partial(\delta Y)}{\partial z} = -R_Y'\delta Y - R_T'\delta T_p \tag{22}$$

Fluid heat balance

$$\frac{\partial(\delta T_f)}{\partial\tau} + \frac{\partial(\delta T_f)}{\partial z} = H(\delta T_p - \delta T_f) + H_w'(\delta T_w - \delta T_f) \tag{23}$$

Catalyst heat balance

$$\frac{\partial(\delta T_p)}{\partial\tau} = H\beta(\delta T_f - \delta T_p) + \beta(R_Y'\delta Y + R_T'\delta T_p) \tag{24}$$

Wall heat balance

$$\frac{\partial(\delta T_w)}{\partial\tau} = H_w'\beta_w(\delta T_f - \delta T_w) - U\beta_w\delta T_w \tag{25}$$

where, in analogy with prior definitions

$$\left.\begin{aligned} R_Y' &= R_s'/Y_s \\ R_T' &= \frac{AT_0}{(T_0+T_{ps})^2}R_s' \\ R_s' &= KY_s\exp\left\{\frac{AT_{ps}}{T_0+T_{ps}}\right\} \end{aligned}\right\} \tag{26}$$

The steady state functions are determined from the equations

$$\frac{dY_s}{dz} = -R_s' \tag{27}$$

$$\frac{dT_{fs}}{dz} = H(T_{ps} - T_{fs}) + H_w'(T_{ws} - T_{fs}) \tag{28}$$

$$0 = H(T_{fs} - T_{ps}) + R_s' \tag{29}$$

$$0 = H_w'(T_{fs} - T_{ws}) - U(T_{ws} - T_{es}) \tag{30}$$

For the conditions of these experiments, further simplifications were possible. Because the value of H was large, catalyst and fluid temperature could be taken to be

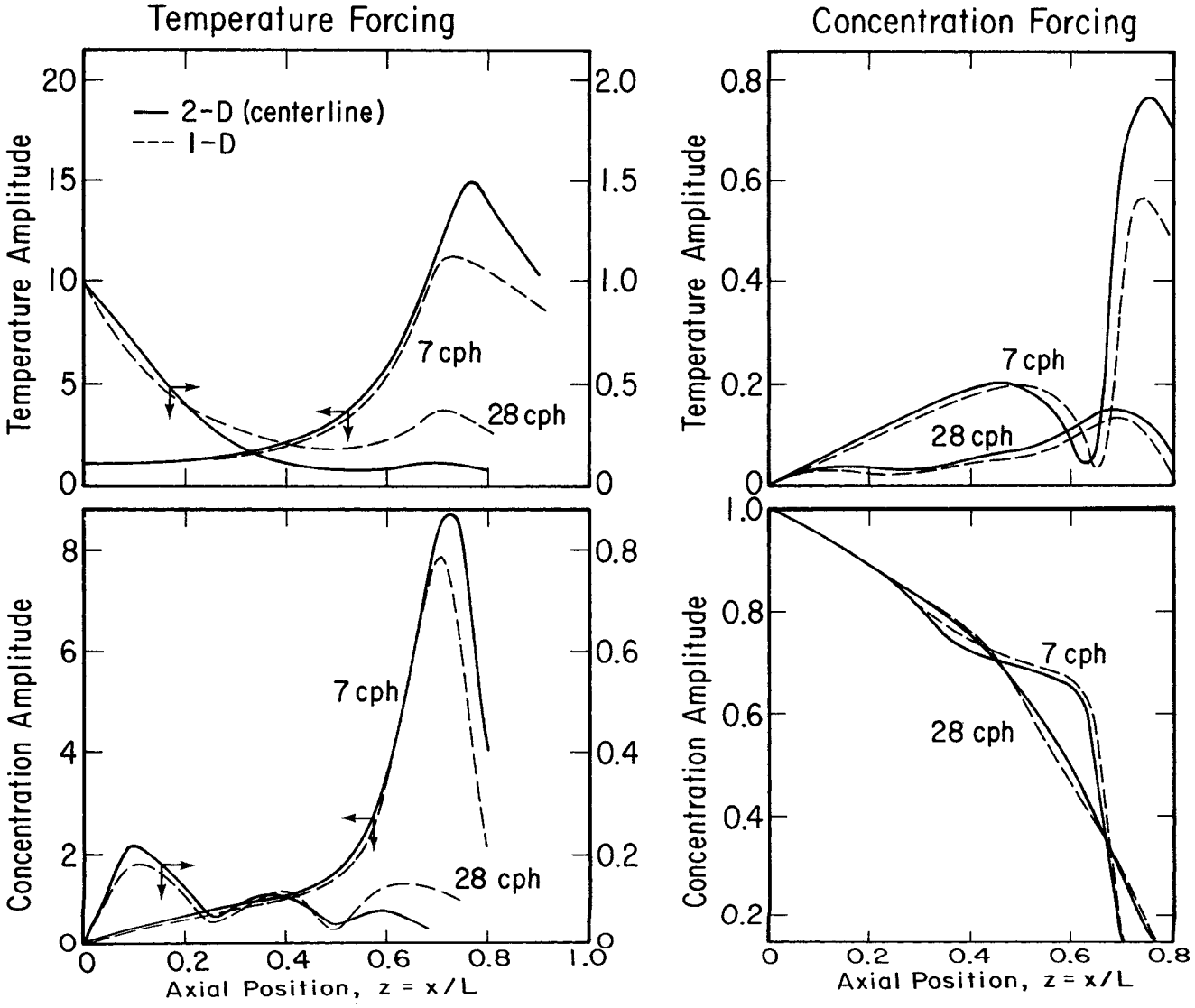

Fig. 7. Comparison of amplitude behavior of the one- and two-dimensional models: small radial gradients.

identical. Furthermore, the mass and heat capacity of the fluid is small, implying that the time derivatives of δY and δT_f in Equations (22) and (23) may be neglected.

In these equations, the heat transfer coefficient H_w' is used with the driving force $(T_f - T_w)$ to represent the rate of radial transport of heat through the bed, and the numerical value of this coefficient is critical to the efficacy of the model. Under transient conditions, H_w' must in general be taken to be a function of time as well as position in order to achieve a perfect match between the fluid temperature of the one-dimensional model and, say, the center-line temperature of the two-dimensional model. Such complexity is undesirable and often unnecessary. Because in the present case the steady state radial heat transfer rate is so important in determining the dynamic behavior, the value of H_w' was considered constant and was determined solely from consideration of the steady state heat transfer process. A good value for H_w' in that case has been shown to be (9)

$$\frac{1}{H_w'} = \frac{Pe_h}{6.133} + \frac{1}{H_w} \tag{31}$$

The behavior of the one-dimensional model using the value of H_w' given by Equation (31) is compared with that of the two-dimensional model in Figure 7. Here, only wave amplitudes at the center line are shown. It is noticed in general that the one-dimensional representation exhibits the major characteristics of the frequency response, but that some discrepancies are evident, particularly in the case of temperature forcing. These discrepancies may be attributed to small differences in the steady state profiles and to differences in the thermal dynamics of the two models. For example, the velocity and dispersion of the waves in the two models differ owing to an inaccurate representation of radial heat flow by the one-dimensional model. When the wall capacitance is small, however, these discrepancies are small, as may be inferred from the results of Amundson (*1*). It may be proposed that the heat transfer coefficient H_w' be selected such that these dynamic discrepancies be minimized, but it is believed that such a determination of H_w' would be incompatable with the need to achieve a close match of the steady state profiles of the two models.

Calculations were also made (*10*) for a case in which the radial temperature difference was about 25% of the absolute temperature level, that is, a gradient an order of magnitude larger than those obtaining in these experiments. The discrepancies between the behavior of the one- and two-dimensional models in this case were quite large, owing principally to a poor match of the steady states. Nonetheless, the one-dimensional model in these cases can be used to indicate the qualitative behavior of the reactor.

CONCLUDING REMARKS

It is clear from these studies that the only dynamic element of consequence in these reactors is the transport of heat at finite rates to and from the stationary thermal capacitances. The other physical and physicochemical processes interact with and are influenced by the heat transport process, of course, but in a way that may be considered nondynamic. The behavior of reactant concentration within a catalyst particle, for example, is seen to be essentially an instantaneous function of the catalyst temperature and the surface concentration. The modeling of the thermal dynamics of the reactor is therefore important, not only because it is the dominant dynamic element, but because the rate of chemical reaction is critically influenced by the state variable of the thermal process, namely, the temperature.

In this modeling the form of the model as well as the parameters of the model are important considerations. It appears that a two-dimensional representation of the heat transport process will be needed when the radial variation of the quantity E/R_gT^* is 20% or more. When this quantity varies only a few percent, a one-dimensional representation of the bed is shown to be of good accuracy. Furthermore, a one-dimensional model may be considered when the values of the heat transfer parameters and the reaction rate parameters are uncertain. While in the present work these parameters were known with reasonable accuracy through independent experiments, it is unlikely that they will be so well known in industrial reactors, and in such cases the one-dimensional model may find application. Many industrial reactors, moreover, will be found with a spectrum of parameters somewhat different from that pertaining to the apparatus used here. Large diameter beds, for example, will have no appreciable radial gradients, and a one-dimensional model will be well suited in such a case. In industrial reactors of small diameter, the ratio of particle diameter to tube diameter will be larger than that used here, with the result that the effective radial thermal conductivity will be larger and the radial temperature gradient smaller in the industrial bed. Such circumstances favor the applicability of a one-dimensional model. Furthermore, in small diameter industrial reactors, the tube wall may often be eliminated as a dynamic element in the model because of high heat transfer rates between the wall and some external cooling or heating medium.

It is remarked that the methods employed here for determination of the parameters are appropriate for modeling the reactor's dynamic behavior but entirely inappropriate for the precise determinations needed in basic studies of transport phenomena and chemical reaction rates. In dynamic modeling, the neglect of second-order effects and the slight confounding of the parameters in the model resulting from their neglect is easily justified. But when the objective of the experiment is the determination of basic phenomenological parameters, second-order effects must be fully accounted for.

There now exists a considerable amount of experimental evidence supporting the applicability of locally linearized, plug-flow, continuum models to fixed-bed reactors with either liquid or gaseous reactants. Models of the same form are found to serve well in either case because of the basic similarity of the behavior in the two cases. The physical process that contributes overwhelmingly to the establishment of this similarity is the heat exchange between fluid and solid. It is this heat exchange that gives birth to propagation velocities different from the fluid velocity, a circumstance that has profound influence on the character of the reactor's dynamic behavior. Thus it appears that models of the form described here may serve as a point of departure for the building of models for more complex reactions, for the investigation of reactor control systems, for the study of still other methods of modeling, and for further theoretical interpretations.

ACKNOWLEDGMENT

This work was performed under grants from the National Science Foundation, and the authors express their appreciation for this support. Some of the calculations were supported by the University of California Computer Center.

Thanks are also extended to R. G. Massard and N. J. Andrade who assisted with some of the calculations reported here.

NOTATION

a = external surface area of catalyst particles per unit volume of bed, ft.$^{-1}$
A = dimensionless activation energy $E/R_gT_i^*$
c_f = heat capacity of fluid, $pcu/$(lb.)(°C.)
c_p = heat capacity of particles
c_w = heat capacity of wall
D_c = effective diffusivity of oxygen in catalyst particle, sq. ft. cat./hr.
D_b = effective radial diffusivity of oxygen in bed, sq. ft. bed/hr.
d_p = particle diameter, ft.
E = activation energy, cal./mole
$f(T_p)$ = $\exp [AT_p/(T_0 + T_p)]$
f_s' = $df_s/dT_{ps} = AT_0 f(T_{ps})/(T_0 + T_{ps})^2$
G_0 = superficial mass flux, $\bar{\rho}_{fi}\,\bar{v}_{fi}\epsilon$, lb./(sq. ft.)(hr.)
h_p = particle-fluid heat transfer coefficient, lb. centigrade unit/(hr.)(sq. ft.)(°C.)
h_w = wall-fluid heat transfer coefficient
h_w' = effective wall-fluid heat transfer coefficient for the one-dimensional model
H, H_w, H_w' = dimensionless heat transfer parameters, h_paL/c_fG_0, $2h_wL/R_1c_fG_0$, and $2h_w'L/R_1c_fG_0$, respectively
j = imaginary unit, $\sqrt{-1}$
k = reaction rate constant, lb.-mole O_2/(lb./sq.ft.abs. $O_2)^n$ (hr.)(cu. ft. bed)
k_e = effective radial thermal conductivity of bed, $pcu/$(hr.)(ft.)(°C.)
k_b = coefficient for the Blake-Kozeny relation, ft.$^{-2}$
K = dimensionless reaction rate constant for two-dimensional model, $k(P_{Ti})^n\ (y_i)^{n-1}\ LM_f \exp(-A)/G_0$
$K_c(z)$ = dimensionless ratio of reaction rate to oxygen diffusivity in catalyst, $\dfrac{kP_T(z)M_fd_p^2 \exp(-A)}{4(1-\epsilon)\epsilon_p\rho_fD_c}$
$K_c'(z)$ = dimensionless reaction rate function for model with diffusional resistance, $3k\,L\,P_T(z)\,M_fe^{-A}/G_0$
K_b = dimensionless coefficient for Blake-Kozeny relation, $k_b\,L\,\bar{\mu}_{fi}\,\bar{v}_{fi}/P_{Ti}$
L = reactor length, ft.
M = molecular weight of oxygen, 32 lb./lb.-mole
M_f = molecular weight of fluid, lb./lb.-mole
n = reaction order with respect to oxygen
Nu = modified Nusselt number, $k_wR_1/k_e = Pe_hH_w/2$
p = absolute partial pressure of oxygen, lb./sq. ft. abs.
P_T = absolute total pressure, lb./sq. ft. abs.
P = dimensionless total pressure, P_T/P_{Ti}
Pe_c = Peclet number for oxygen transport in catalyst particle, $d_pG_0/2\epsilon_p\rho_fD_cLa$
Pe_h = modified Peclet number for radial heat transport in bed, $R_1^2c_fG_0/k_eL$
Pe_m = modified Peclet number for radial mass transport in bed, $R_1^2G_0/\rho_fD_bL$
q_h = radial heat flux, $pcu/$(hr.)(sq. ft.)
q_m = radial mass flux, lb. O_2/(hr.)(sq. ft.)
r = radial coordinate, ft.
r = dimensionless radial coordinate, r/R_1
r_η = sensitivity of reaction rate to catalyst oyxgen concentration, K_cf_s
r_T = sensitivity of reaction rate to catalyst temperature, $K_cf_s'\eta_s$
R_1 = radius of inner surface of tube wall, ft.
R_2 = radius of outer surface of tube wall, ft.
R_g = universal gas constant, 1.987 cal./(g.-mole)(°K.)
Re = Reynolds number, $d_p\rho_fv_f/\mu_f$
R = dimensionless reaction rate, $KP^nY^n \exp [AT_p/(T_0 + T_p)]$
R^* = reaction rate, $k\,p^n \exp(-E/R_gT_p^*)$
R' = dimensionless reaction rate for the 1-D model, $KY \exp [AT_p/(T_0 + T_p)]$
R_P = sensitivity of reaction rate to total pressure, $\partial R_s/\partial P_s = nR_s/P_s$
R_T = sensitivity of reaction rate to catalyst temperature, $\partial R_s/\partial T_{ps} = R_sAT_0/(T_0 + T_p)^2$
R_Y = sensitivity of reaction rate to concentration $\partial R_s/\partial Y_s = nR_s/Y_s$
R_T', R_Y' = sensitivity of reaction rate for 1-D model to catalyst temperature and concentration, respectively
s = complex variable from the Laplace transformation
t = time, hr.
$T_e^*, T_f^*, T_p^*, T_w^*$ = absolute temperature of room, fluid, particles, and wall, respectively, °K.
T_i^* = constant reference temperature that is representative of the feed temperature, °K.
T_e, T_f, T_p, T_w = dimensionless temperatures of room, fluid, particle, and wall, respectively, $(T_e^* - T_i^*)/\Delta T_a$, etc.
T_0 = dimensionless reference temperature $T_i^*/\Delta T_a$
U^* = wall-surroundings heat transfer coefficient, $pcu/$(hr.)(sq. ft.)(°C.)
U = dimensionless wall-surroundings heat transfer coefficient, $2U^*\ R_2L/R_1^2c_fG_0$
v_f = interstitial velocity of fluid, $v_f = v_xv_r$, ft./hr.
v_r = radial dependence of fluid velocity (normalized by $2\int_0^{R_1} rv_{fr}\,dr = R_1^2$
v_x = interstitial velocity averaged across the radius, $2\int_0^{R_1} rv_f dr/R_1^2$
v = dimensional fluid velocity, $v_f/\bar{v}_{fi}$
$\bar{v}_{fi}$ = radially averaged fluid velocity at reactor inlet, ft./hr.
v_r = radial dependence of velocity as a function of dimensionless radial coordinate, $v_r(r)$
v_z = dimensionless radial average of interstitial velocity, $v_x/\bar{v}_{fi}$
w = mass fraction of oxygen in fluid
x = axial coordinate, ft.
y = mole fraction of oxygen in fluid, wM_f/M
y_i = constant reference oxygen mole fraction that is representative of the feed
Y = normalized oxygen mole fraction, y/y_i
z = dimensionless axial coordinate, x/L

Greek Letters

α, α_1 = $\sqrt{r_\eta}$ and $\sqrt{r_\eta + \phi s}$, respectively
β, β_w = dimensionless thermal capacity ratios, respectively, $\epsilon c_f\bar{\rho}_{fi}/(1-\epsilon)c_p\rho_p$, $\epsilon c_f\bar{\rho}_{fi}R_1^2/c_w\rho_w(R_2^2 - R_1^2)$
$\delta P, \delta\eta, \delta\rho, \delta T_f, \delta T_p, \delta T_w, \delta v, \delta Y$ = respectively, deviations from steady state pressure, catalyst oxygen concentration, density, fluid temperature, particle temperature, wall temperature, fluid velocity, and oxygen concentration, $(P - P_s)$, $(\eta - \eta_s)$, etc.
$(-\Delta H)$ = heat of reaction, pcu/lb.-mole O_2
ΔT_a = adiabatic temperature rise, $y_i\,(-\Delta H)/c_fM_f$
ϵ = void fraction of bed
ϵ_p = void fraction of an individual catalyst particle
η = normalized oxygen mole fraction in fluid in catalyst pores
μ_f = viscosity of fluid, (lb.$_f$)(hr.)/sq. ft.
μ = dimensionless fluid viscosity, $\mu_f/\bar{\mu}_{fi}$
ξ = dimensionless radial coordinate for catalyst particle

ρ_f = density of fluid, lb./cu. ft.
ρ_p = apparent density of catalyst particles, lb./cu. ft.
ρ_w = density of tube wall, lb./cu. ft.
ρ = dimensionless fluid density, ρ_f/ρ_{f_i}
τ = dimensionless time, $t\ \bar{v}_{fi}/L$
ϕ = $d_p^2\ \bar{v}_{fi}/4D_cL$
ω = dimensionless frequency

Subscripts

s = steady state value of variable
f = fluid
p = particle
w = wall
i = constant reference value at inlet

Superscripts

— = average across radius
0 = boundary condition at $z = 0$

LITERATURE CITED

1. Amundson, N. R., *Ind. Eng. Chem.*, **48**, 26 (1956).
2. Ball, W. E., Ph.D. thesis, Washington Univ., St. Louis, Mo. (1958).
3. Benesi, H. A., R. M. Curtis, and H. P. Studer, *J. Catalysis*, **10**, 328 (1968).
4. Boreskov, G. K., and M. G. Slin'ko, *Pure Appl. Chem.*, **10**, 611 (1965).
5. Carberry, J. J., and Donald White, *Ind. Eng. Chem.*, **61** (7), 27 (1969).
6. Cowles, J. O., Ph.D. thesis, Univ. Michigan, Ann Arbor (1963).
7. Crider, J. E., and A. S. Foss, *AIChE J.*, **14**, 77 (1968).
8. *Ibid.*, **12**, 514 (1966).
9. *Ibid.*, **11**, 1012 (1965).
10. Hoiberg J. A., Ph.D. thesis, Univ. California, Berkeley (1969).
11. Hougen, O. A., K. M. Watson, and R. A. Ragatz, "Chemical Process Principles," Pt. I, p. 373, Wiley, New York (1959).
12. Lyche, B. C., Ph.D. thesis, Univ. California, Berkeley (1968).
13. Massard, R. G., M.S. thesis, Univ. California, Berkeley (1967).
14. Maymo, J. A., and J. M. Smith, *AIChE J.*, **12**, 845 (1966).
15. Miller, F. W., and H. A. Deans, *ibid.*, **13**, 45 (1967).
16. Schwartz, C. E., and J. M. Smith, *Ind. Eng. Chem.*, **45**, 1209 (1953).
17. Simpkins, R. C., Ph.D. thesis, Univ. Delaware, Newark (1965).
18. Sinai, José and A. S. Foss, *AIChE J.*, **16**, 658 (1970).
19. Tinkler, J. E., and D. E. Lamb, *Chem. Eng. Progr. Symp. Ser., No. 55*, **61**, 155 (1965).
20. Von Rosenberg, D. U., P. L. Durrill, and E. H. Spencer, *Brit. Chem. Eng.*, **7**, 186 (1962).

APPENDIX: A ONE-DIMENSIONAL MODEL ACCOUNTING FOR TRANSPORT RESISTANCE WITHIN CATALYST

The assumptions are similar to those stated for the two-dimensional model with the exception that only a first-order reaction is considered. The catalyst is considered to be spherical and the conditions within it spherically symmetric.

Only equations in the normalized form are presented, the normalization of the variables being identical to that employed for the two-dimensional model.

Total mass balance for fluid

$$\frac{\partial \rho}{\partial \tau} + \frac{\partial(\rho v)}{\partial z} = 0 \qquad (A1)$$

Oxygen balance for fluid

$$\rho \frac{\partial Y}{\partial \tau} + \rho v \frac{\partial Y}{\partial z} = -\frac{1}{Pe_c} \frac{\partial \eta}{\partial \xi}\bigg|_{\xi=1} \qquad (A2)$$

Heat balance for fluid

$$\rho \frac{\partial T_f}{\partial \tau} + \rho v \frac{\partial T_f}{\partial z} = H(T_p - T_f) + H_w'(T_w - T_f) \qquad (A3)$$

Heat balance for wall

$$\frac{\partial T_w}{\partial \tau} = H_w'\beta_w\,(T_f - T_w) - U\beta_w\,(T_w - T_e) \qquad (A4)$$

Oxygen balance for the catalyst

$$\frac{\partial^2 \eta}{\partial \xi^2} + \frac{2}{\xi}\frac{\partial \eta}{\partial \xi} - \phi \frac{\partial \eta}{\partial \tau} = K_c(z)\ f(T_p)\eta \qquad (A5)$$

Boundary conditions

$$\frac{\partial \eta}{\partial \xi}\bigg|_{\xi=0} = 0; \qquad \eta(0, \tau, z) = Y(\tau, z)$$

Heat balance for catalyst

$$\frac{\partial T_p}{\partial \tau} = H\beta(T_f - T_p) + \beta K_c'\, f(T_p) \int_0^1 \eta(\xi)\xi^2 d\xi \qquad (A6)$$

Representations of the equation of state and fluid pressure drop are similar to those given for the two-dimensional model.

The linearization of these relations for small deviations about the steady state is performed in a straightforward manner similar to that shown earlier and is not shown here. Some special relations, however, are given for the catalyst.

The steady state concentration profile within the catalyst is obtained by solution of Equation (A5) with the time derivative set to zero.

$$\eta_s = \frac{\sinh(\alpha\xi)}{\xi \sinh \alpha} Y_s(z) \qquad (A7)$$

Linearization of Equation (A5) about η_s gives

$$\frac{\partial^2(\delta\eta)}{\partial \xi^2} + \frac{2}{\xi}\frac{\partial(\delta\eta)}{\partial \xi} - \phi \frac{\partial(\delta\eta)}{\partial \tau} = r_\eta\ \delta\eta + r_T\ \delta T_p \qquad (A8)$$

and solution for the Laplace transformation of $\delta\eta$ gives

$$\delta\eta(\xi, s, z) = \frac{\sinh \alpha_1 \xi}{\xi \sinh \alpha_1}\,\delta Y(s, z) + \frac{K_c f_s' Y_s}{\phi s}\left[\frac{\sinh \alpha_1 \xi}{\xi \sinh \alpha_1} - \frac{\sinh \alpha\xi}{\xi \sinh \alpha}\right]\delta T_p(s, z) \qquad (A9)$$

where

$$\alpha^2 = r_\eta = K_c(z)\ f(T_p)$$
$$\alpha_1^2 = r_\eta + \phi s$$

From this expression, relationships can be obtained for the Laplace transformation of the concentration gradient $\partial(\delta\eta)/\partial\xi|_1$ needed in the linearized version of Equation (A2) and also for the integral in the linearized version of Equation (A6). These are (*13*)

$$\frac{\partial(\delta\eta)}{\partial \xi}\bigg|_1 = (\alpha_1 \coth \alpha_1 - 1)\ \delta Y(s, z) + \frac{K_c f_s' Y_s}{\phi s}\left[\alpha_1 \coth \alpha_1 - \alpha \coth \alpha\right]\delta T_p(s, z) \qquad (A10)$$

and

$$\int_0^1 \delta\eta\xi^2 d\xi = \left[\frac{\coth \alpha}{\alpha} - \frac{1}{\alpha^2}\right]\delta Y(s, z) + \frac{K_c f_s' Y_s}{\phi s}\left[\frac{\coth \alpha_1}{\alpha_1} - \frac{1}{\alpha_1^2} - \frac{\coth \alpha}{\alpha} + \frac{1}{\alpha^2}\right]\delta T_p(s, z) \qquad (A11)$$

Manuscript received May 25, 1970; revision received September 11, 1970; paper accepted November 12, 1970.